Available online at www.sciencedirect.com
SCIENCE DIRECT®
Journal of Nuclear Materials 329–333 (2004) 830–835
journal of nuclear materials
www.elsevier.com/locate/jnucmat

# Simulation study of sputtering erosion and impurity deposition on carbon and tungsten surfaces irradiated with deuterium plasmas including carbon impurity

T. Mitani, R. Kawakami *, S. Kuriu

*Faculty of Engineering, The University of Tokushima, Tokushima 770-8506, Japan*

**Abstract**

Sputtering erosion and impurity deposition on C and W surfaces irradiated with $D^+$ plasmas containing $C^{4+}$ impurity have been studied. For the C target, the net erosion is suppressed by the local redeposition resulting from charge exchange reactions of chemically sputtered $CD_x$ with $D^+$ at the high plasma density and low plasma temperature. The D/XB values for $CD_4$ reaction chains with electrons plus deuterium ions are lower than those for $CD_4$ reaction chains with electrons at the low temperature. At the high temperature, these D/XB values which reproduce the experimental data are almost the same. For the W target, in association with the $C^{4+}$ impurity concentration, the erosion and deposition occur near to and far from the LCFS, respectively, which qualitatively reproduces the experimental data. The erosion and deposition fluctuate depending on the target temperature. The fluctuation is explained by an interrelation between the diffusion and the reflective scattering collision.


## 1. Introduction

In the ITER divertor, carbon (C) and tungsten (W) materials are simultaneously used as plasma facing materials [1]. Because of their advantageous points, the C material has a high thermal shock resistance and the W material has a low erosion rate. However, due to chemical sputtering resulting from chemical reactivity with deuterium (D) plasmas via formation of methane ($CD_4$), the C material is eroded easily. The C erosion brings about contamination of the plasmas with a C impurity concentration of a few percent or less in the current ITER design [2]. During exposure to the plasmas including C impurity, erosion of the W material and deposition of the C impurity on the W material result [3]. This complicates prediction of the net erosion of W material. For the C material, the similar problem occurs. Thus, there is a strong concern how the contaminated D plasma exposure influences the net erosion of both C and W materials.

In this study, the influence of chemical erosion of C targets associated with the transport of eroded $CD_4$ in the edge plasmas has been studied using a plasma-surface interaction code, EDDY [4,5]. Also, the net erosion of W targets at elevated temperatures when irradiated with D plasmas including C impurity has been studied. The code calculates net erosion, including not only redeposition of physically and chemically sputtered impurities but also thermal diffusion of impurities deposited on the target. The paper describes changes in net erosion of the C targets as functions of various edge plasma temperature and density. Emphasis is put on a difference in the net erosion between $CD_4$ reaction chains with electrons and those with electrons plus deuterium ions in the edge plasma. The paper also describes a dependence of net erosion of the W targets on

* Corresponding author. Tel./fax: +81-88 656 7441.
*E-mail address:* retsuo@ee.tokushima-u.ac.jp (R. Kawakami).

0022-3115/$ - see front matter © 2004 Elsevier B.V. All rights reserved.
doi:10.1016/j.jnucmat.2004.04.212

the various target temperature. These results are compared with experimental data obtained in TEXTOR-94 [3,6].

## 2. Simulation code for interactions between edge plasmas and targets

Based on the binary collision model [7] and the Monte Carlo impurity transport model [8], net erosion of targets at elevated temperatures irradiated with the edge plasma is calculated by EDDY. The energy of plasma ions impinging on the target is given by the drifting Maxwellian distribution with an acceleration energy due to the electrostatic sheath potential of $V_s = (kT_e/2e)\ln(2\pi\{m_e/m_i\}\{1 + T_i/T_e\})$ [9]. Here, $T_e$ and $T_i$ are plasma electron and ion temperatures in front of the targets, respectively, $m_e$ is the electron mass and $m_i$ is the ion mass. For the targets, local atomic composition changes near the surfaces due to collision cascades by moving particles and thermal diffusion of impurities deposited on the target are simulated in the same manner as TRIDYN/PIDAT [10]. From the local atomic composition changes, a decrease (erosion) or an increase (deposition) in the thickness of the target is calculated. The thickness of the deposited C is simply calculated using the density of C element ($1.136\times10^{23}$ $cm^{-3}$).

For the edge plasmas, impurities released from the surfaces by physical sputtering (C release or W release) and chemical sputtering ($CD_4$ release) are followed based on the Lorentz force motion, including the ionization and dissociation reactions with electrons as well as the ionization reactions with deuterium ions. The released impurities are assumed to leave the surfaces as neutrals. The ionization and dissociation events are modeled using their rate coefficients for proton ($P^+$) and $CH_4$, instead of $D^+$ and $CD_4$ [11]. The use is based on the assumption that there would not be a significant difference in atomic and molecular processes between $D^+$ and $P^+$ and in those between $CD_4$ and $CH_4$. In the modeling, the ionized particles are subjected to gyromotion with collisional friction forces parallel to the magnetic field. The dissociated particles are scattered isotropically with an additional energy by the Frank–Condon principle. The simulation is performed until the released particles are either redeposited on the targets or leave the calculation volume. The sticking coefficient of the hydrocarbons hitting the target is assumed to be 100%. The contribution of background hydrocarbons from the next to the calculation volume is neglected because it is weaker than that of C impurity transported by a plasma from other wall targets. Details of EDDY have been described elsewhere [4,5].

## 3. Results and discussion

### 3.1. Net erosion of carbon targets irradiated with edge plasmas

For the simulation, experimental conditions for a spherically shaped C test limiter irradiated with the TEXTOR-94 edge plasmas has been used. The top of the test limiter, 10 cm long in the toroidal direction and 8.5 cm wide in the poloidal direction, is located at the last closed flux surface, the LCFS (at a minor radius of $r \sim 46$ cm). Details of the experiment have been described in Ref. [6]. The radial profiles of edge plasma density and temperature fitted exponentially to those measured by the Li-and He-diagnostics are used: their e-folding lengths are 2.0 and 2.5 cm, respectively [12,13]. The density and temperature at the LCFS, $n_{eLCFS}$ and $T_{eLCFS}$, are variable. Based on features of the TEXTOR-94 edge plasmas, $D^+$ and $C^{4+}$ are used assuming $T_i = T_e$ [14]. The flux ratio C/D, which decreases from 2.0% to 4.4% with increasing $r$ from the LCFS to 49.5 cm, is used [15]. The target temperature of 600 K (0.05 eV) is assumed.

A change in erosion and deposition rates of the C target at $r = 47$ cm, which is 30° from the toroidal magnetic field, with $n_{eLCFS}$ and $T_{eLCFS}$ is calculated as shown in Fig. 1. For no chemical sputtering, with increasing $T_{eLCFS}$, the deposition rate at a low density of $n_{eLCFS} = 10^{12}$ $cm^{-3}$ increases to a maximum, returns to zero, and changes to erosion (Fig. 1(a)). For a high density of $n_{eLCFS} = 10^{13}$ $cm^{-3}$, a similar trend arises, but the erosion and deposition rates are ten times higher (Fig. 1(b)). The deposition is because reflection of the C impurity and physical sputtering of the target do not occur due to the low plasma temperatures. The increase in the deposition rate is because the impinging flux increases in proportion to $n_e T_e^{1/2}$. The erosion is due to a significant contribution of the physical sputtering resulting from the high plasma temperature.

The addition of the chemical sputtering decreases the deposition rate, and it increases the erosion rate. When the chemical sputtering yield $Y_{CD4}$ increases to 0.04, the erosion occurs even at $T_{eLCFS} < 10$ eV (Fig. 1(a) and (b)). The figure also shows that the erosion rate relates to reaction of eroded $CD_4$ with the plasmas, which influence their local and prompt redeposition. For low density, there is little difference in the erosion rate between $CD_4$ reaction chains with electrons and those with electrons plus deuterium ions in the plasmas (Fig. 1(a)). For high density, however, a different trend arises (Fig. 1(b)). The erosion rate is decreased by the additional reactions with deuterium ions (the charge exchange reactions with deuterium ions: $D^+ + CD_x \rightarrow CD_x^+ + D$ for $x = 1$–4 and $D^+ + C \rightarrow C^+ + D$). At $T_{eLCFS} < 10$ eV, the erosion rate for the additional reactions with deuterium ions is half that for $CD_4$ reaction chains with

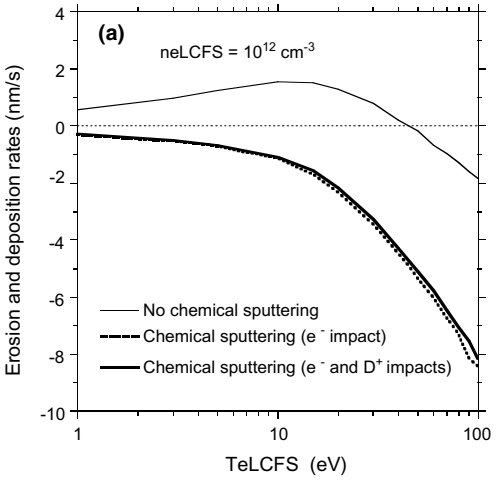


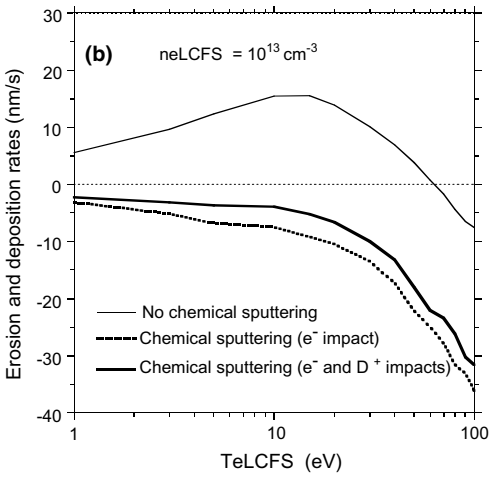


Fig. 1. Erosion and deposition rates of a C target irradiated with $D^+$ plasmas including $C^{4+}$ impurity (C: 2.5%) for different plasma temperatures at LCFS, $T_{eLCFS}$, at plasma densities at LCFS of (a) $n_{eLCFS} = 10^{12}$ cm$^{-3}$ and (b) $n_{eLCFS} = 10^{13}$ cm$^{-3}$. The chemical sputtering yield $Y_{CD_4}$ is assumed to be $Y_{CD_4} = 0.04$. On the vertical axes, plus and minus signs indicate the deposition rate and the erosion rate, respectively. Thick dotted and solid curves correspond to the results for $CD_4$ reaction chains with electrons and those with electrons plus deuterium ions in the plasmas, respectively.

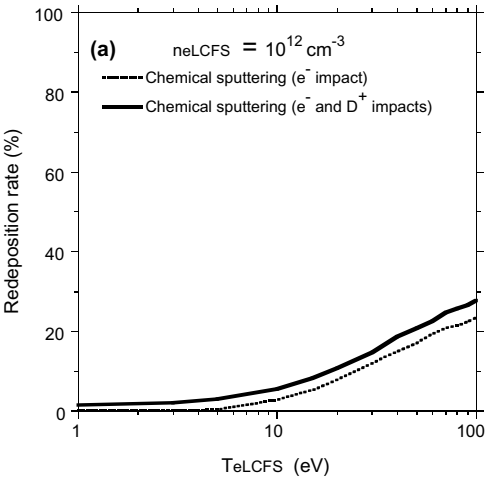


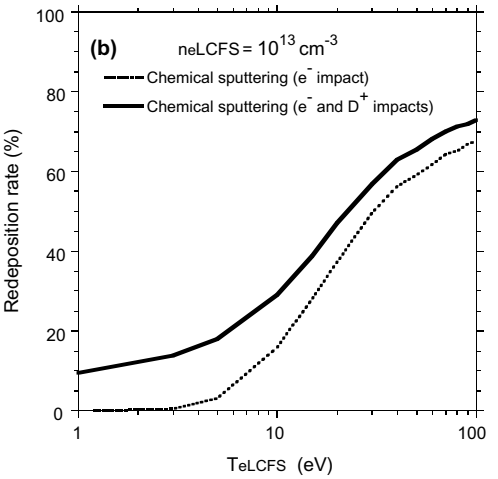


Fig. 2. Redeposition rates of chemically sputtered particles, as a function of $T_{eLCFS}$, for $CD_4$ reaction chains with electrons (dotted curves) and those with electrons plus deuterium ions (solid curves), at (a) $n_{eLCFS} = 10^{12}$ cm$^{-3}$ and (b) $n_{eLCFS} = 10^{13}$ cm$^{-3}$. On the vertical axes, 0% means that no chemically sputtered particles are redeposited promptly and locally on the target. Other notations are the same as those used in Fig. 1.

electrons. This decrease is explained using a redeposition rate defined by a rate of locally redeposited particles to chemically sputtered particles. For $n_{eLCFS} = 10^{12}$ cm$^{-3}$, the redeposition rates for the two reaction chains are almost the same, and at $T_{eLCFS} < 10$ eV they are close to 0% (Fig. 2(a)). For $n_{eLCFS} = 10^{13}$ cm$^{-3}$, however, the redeposition rate for the additional reactions with deuterium ions at $T_{eLCFS} < 10$ eV is increased (Fig. 2(b)), which results in the decrease in the erosion rate. This reason is that, at $n_{eLCFS} = 10^{13}$ cm$^{-3}$ and $T_{eLCFS} < 10$ eV, the charge exchange reactions of hydrocarbons with deuterium ions are more pronounced, and the ionized particles are easily redeposited by the magnetic field directed to the target. From the result, net erosion of C targets irradiated with the detached plasma in the divertor is expected to be significantly compensated by the local redeposition resulting from the charge exchange reactions with deuterium ions.

In general, for measurement of the chemical sputtering yield, the D/XB value which is defined by a ratio of the $CD_4$ flux to the intensity of the CD band emission (430 nm) is used [15]. As shown in Fig. 3(a), at $n_{eLCFS} = 10^{12}$ cm$^{-3}$ and $T_{eLCFS} > 10$ eV, the D/XB values

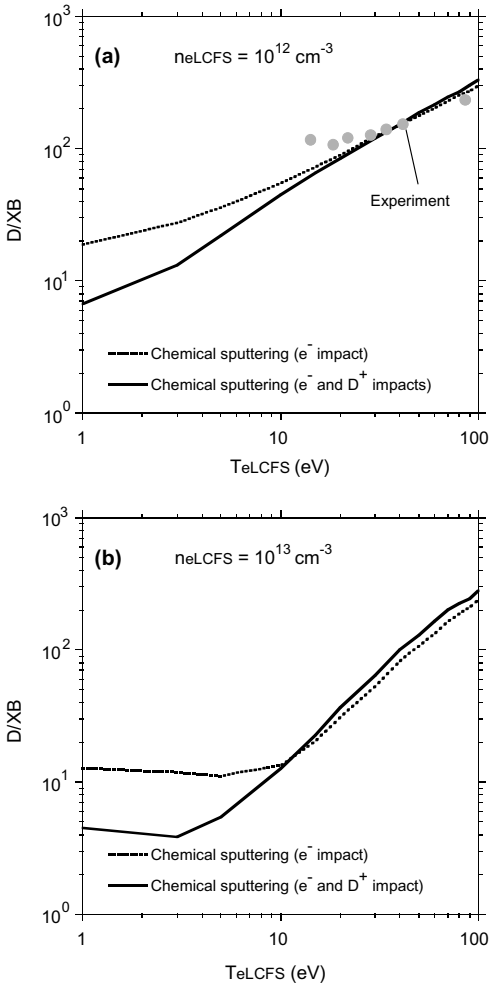


Fig. 3. D/XB values of CD from eroded $CD_4$, as a function of $T_{eLCFS}$, for $CD_4$ reaction chains with electrons (dotted curves) and those with electrons plus deuterium ions (solid curves), at (a) $n_{eLCFS} = 10^{12}$ cm$^{-3}$ and (b) $n_{eLCFS} = 10^{13}$ cm$^{-3}$. Solid circles correspond to the experimental data obtained in TEXTOR-94 [6]. Other notations are the same as those used in Fig. 1.

for the two reaction chains are almost the same. They increase with $T_{eLCFS}$ because the hydrocarbons are redeposited promptly and locally before becoming CD radicals. The result is in good agreement with the TEXTOR-94 data [6]. This agreement indicates that there is little influence of the additional reactions with deuterium ions on the D/XB values at $T_{eLCFS} > 10$ eV. For $n_{eLCFS} = 10^{13}$ cm$^{-3}$ and $T_{eLCFS} > 10$ eV, there is the similar trend as shown in Fig. 3(b), but the D/XB values increases more steeply due to the higher redeposition rates of Fig. 2(b). However, there is a difference in the D/XB values between the two reaction chains at $T_{eLCFS} < 10$ eV. The D/XB value for the additional reactions with deuterium ions is lower. The trend is more pronounced at high density. This is because the hydrocarbons can change to CD radicals by additional reactions with deuterium ions. The result indicates that, at low temperature, the D/XB value is strongly dependent on the $CD_4$ reaction chains.

### 3.2. Net erosion of tungsten targets irradiated with edge plasmas

For the simulation, experimental conditions for a W layer 300 nm in thickness on a graphite sample, which is at 20° to the toroidal magnetic field and irradiated with the TEXTOR-94 edge plasmas have been used. Details of the experiment have been described in [3]. Similarly, the exponentially fitted density and temperature are used: $n_{eLCFS}$ is $2\times10^{12}$ cm$^{-3}$, $T_{eLCFS}$ is 50 eV, and their e-folding lengths are 2.55 and 7.5 cm, respectively. The features of the TEXTOR-94 edge plasmas described earlier are used.

The temporal evolution of erosion and deposition on a W target exposed near to the LCFS, at $r = 49$ cm, for different target temperatures, $T$, is simulated as shown in Fig. 4(a). The result is calculated using the diffusion coefficient measured by other experiments for thermal diffusion of C in W, $D_0 = 3.15 \times 10^{-7}$ m$^2$/s and $Q = 1.78$ eV [16]. If diffusion is not taken into account, the target is eroded due to the high plasma temperature and low C impurity concentration. However, the addition of diffusion causes a change from the erosion to deposition (Fig. 4(a)). With increasing temperature, the erosion is slightly enhanced ($T < 950$ K), but it is suppressed and then changes to deposition due to deep penetration of the deposited C atoms in the W target by diffusion ($T > 950$ K). The enhancement of erosion is explained by an increase in physical sputtering of the deposited C atoms, which results from the reflective scattering collisions at W–C mixed layers near the surface [17].

For a W target exposed far from the LCFS (at $r = 50.1$ cm), there is a different temperature dependence of the erosion and deposition, as shown in Fig. 4(b). With increasing exposure time, a transition from erosion to deposition occurs if no diffusion is taken into account. This transition is due to the low plasma temperature and high C impurity concentration. The depth profile for no diffusion shows formation of a C film on the target (not shown here). As the temperature increases ($T < 600$ K), the amount of deposition is increased by diffusion. At temperatures above 600 K, deposition is suppressed, and eventually, erosion occurs. The result is explained by an interrelation between diffusion and the reflective scattering collisions. By the significant contribution of diffusion, the deposited C atoms penetrate more deeply, which results in formation or growth of a W–C mixed layer near the surface. As a result, since the reflective scattering collision occurs easily, physical sputtering of the deposited C atoms is enhanced by additional

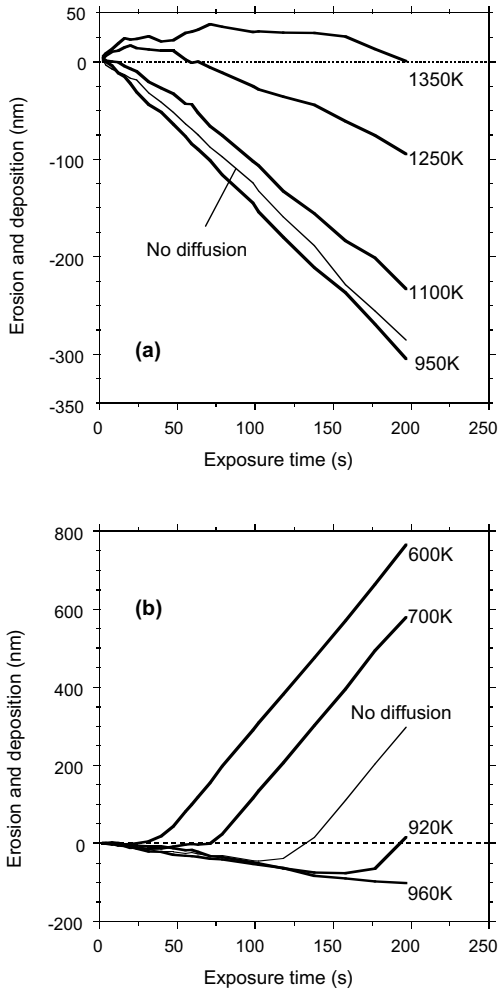


Fig. 4. Temporal evolution of erosion and deposition on W targets irradiated with $D^+$ plasma including $C^{4+}$ impurity for different target temperatures. (a) and (b) show the results near and far the LCFS, respectively. On the vertical axes, plus and minus signs indicate deposition of C impurity and erosion of the target, respectively. Thin curves correspond to the results calculated by taking no diffusion into account.

emission of the C atoms due to impact of D ions reflected from the W atoms. Physical sputtering of the W atoms is also enhanced because of the decrease in the deposited C atoms (due to no protection layer of the C atoms on the W target).

A comparison between Fig. 4(a) and (b) indicates that there is erosion at $T < 1350$ K on the target near to the LCFS, whereas there is deposition at $T < 930$ K on the target far from the LCFS. This result qualitatively reproduces the TEXTOR-94 experimental data [3]. From the agreement, the erosion and deposition on the W targets is found to fluctuate significantly in response to the plasma temperature, the plasma density and the target temperature. For the calculation, a choice of the diffusion coefficient is a crucial issue. If using the smaller diffusion coefficient, there may not be a significant change of the thickness at the given target temperatures.

## 4. Conclusions

Sputtering erosion and impurity deposition on C and W surfaces irradiated with $D^+$ plasmas containing $C^{4+}$ impurity have been studied using the EDDY simulation code for plasma–surface interactions. For the C target, emphasis is put on a difference in the net erosion between $CD_4$ reaction chains with electrons and those with electrons plus deuterium ions in the plasma. At high plasma density and low plasma temperature, net erosion is significantly suppressed by the local redeposition resulting from the charge exchange reactions of chemically sputtered $CD_x$ molecules with deuterium ions. The D/XB values for the two $CD_4$ reaction chains are not the same at the low temperature, whereas at the high temperature the D/XB values which reproduce the experimental data are independent of the $CD_4$ reaction chains. For the W target, emphasis is put on temporal evolutions of the erosion and deposition on the targets near to and far from the LCFS. In association with the C impurity concentration, erosion occurs near to LCFS, and deposition occurs far from the LCFS, which qualitatively reproduces the TEXTOR experimental data. The erosion and deposition fluctuate depending on the target temperature. Their temperature dependences differ, which is explained by an interrelation between the diffusion and the reflective scattering collision.

## References

[1] ITER Physics Expert Group on Divertor Modeling and Database, ITER Physics Basis Editors, Nucl. Fusion 39 (1999) 2391.
[2] V. Philipps, T. Tanabe, Y. Ueda, A. Pospieszczyk, M.Z. Tokar, B. Unterberg, L. Konen, B. Schweer, U. Samm, P. Wienhold, J. Winter, M. Rubel, B. Emmoth, N.C. Hawkes, Nucl. Fusion 34 (1994) 1417.
[3] D. Hildebrandt, P. Wienhold, W. Schneider, J. Nucl. Mater. 290–293 (2001) 89.
[4] R. Kawakami, K. Ohya, Jpn. J. Appl. Phys. 42 (2003) 3623.
[5] R. Kawakami, K. Ohya, Jpn. J. Appl. Phys. 42 (2003) 5259.
[6] A. Pospieszczyk, V. Philipps, E. Casarotto, U. Kögler, B. Schweer, B. Unterberg, F. Weschenfelder, J. Nucl. Mater. 241–243 (1997) 833.
[7] W. Möller, W. Eckstein, J.P. Biersack, Comput. Phys. Commun. 51 (1988) 355.

[8] D. Naujoks, Nucl. Fusion 33 (1993) 581.
[9] P.C. Stangeby, The plasma sheath, in: D.E. Post, R. Behrisch (Eds.), Physics of Plasma-Wall Interactions in Controlled Fusion, Plenum, New York, 1985, p. 55.
[10] W. Eckstein, V.I. Shulga, J. Roth, Nucl. Instrum. and Meth. B 153 (1999) 415.
[11] A.B. Ehrhardt, W.D. Langer, Rep. Princeton Plasma Phys. Lab., PPPL-2477, 1986.
[12] M. Brix, Report of IPP Jülich, Jül-3638, 1998.
[13] A. Kirschner, V. Philipps, A. Pospieszczyk, P. Wienhold, Phys. Scr. T 91 (2001) 57.
[14] M.Z. Tokar, Plasma Phys. Contr. Fusion 36 (1994) 1819.
[15] D. Naujoks, D. Coster, H. Kastelewicz, R. Schneider, J. Nucl. Mater. 266–269 (1999) 360.
[16] V.Y. Shchelkonogov, L.N. Aleksandrov, V.A. Piterimov, V.S. Mordyuk, Phys. Met. Metallogr. 25 (1968) 68.
[17] R. Kawakami, K. Ohya, Jpn. J. Appl. Phys. 40 (2001) 6581.